# Photofragmentation of Mass-Resolved $Si_{2-12}^{+}$ Clusters

L. A. Bloomfield, R. R. Freeman, and W. L. Brown
*AT&T Bell Laboratories, Murray Hill, New Jersey 07974*
(Received 19 February 1985)

The photofragmentation spectra of $Si_n^+$ for $n = 2$ to 12 have been obtained in an apparatus that produces, isolates, and fragments ionic clusters on a mass-resolved basis. The most prominent species are found to be $Si_6^+$ and $Si_{10}^+$. The fragmentation data are shown to be consistent with a microcrystal model of cluster geometry for $Si_n^+$.

PACS numbers: 61.90.+d, 33.80.−b, 36.40.+d

"Magic numbers" have been identified in the relative populations of aggregates between 2 and 150 atoms in recent studies of small metal, semiconductor, and noble-gas clusters.[1–8] These magic numbers have been attributed to geometry,[4,5] maximal bond number,[2] and electronic structure.[7] In a typical experiment designed to measure the relative abundances of cluster sizes, a collection of neutral aggregates with differing masses is ionized, and the resulting ionic clusters are then mass separated and counted. Even in the event that the ionization-efficiency and detection-probability functions of the equipment are well understood, fragmentation can make the correspondence between a strong cluster-ion signal and a "magic" neutral-cluster size uncertain. Fragmentation can compete with ionization under many experimental conditions,[9] especially when the fluence of the ionizing agent is large, because as we show, fragmentation cross sections are comparable to large photoionization cross sections.

The ambiguities associated with ionization may be avoided either by growing preionized clusters, as has been demonstrated very recently,[2] or by studying the properties of clusters *after* they have been both ionized *and* mass selected.[10,11] In this Letter, we describe results for Si using the latter type of measurement. Our experiments produce $Si^+$ clusters as large as 150 atoms, but the results reported here are limited to photofragmentation of $Si_n^+$ microclusters for $n = 2$ to 12. Analysis of the photofragmentation cross sections and branching ratios as a function of initial cluster ion mass show $Si_6^+$ to be an unusually stable ionic cluster. On the basis of a simple model, geometries for $Si_n^+$ clusters for $n$ greater than 6 are also suggested.

The apparatus for these studies is shown in Fig. 1 and makes use of a pulsed source of clusters, pulsed ionization and fragmentation lasers, and time-of-flight techniques to isolate a given cluster size. The inset shows the timing sequence of the experiment. The apparatus is cycled at 10 Hz, and the complete mass scan for each shot is accumulated by a 200-MHz transient digitizer.

The neutral clusters, produced in a pulsed-laser-vaporization expansion source following Hopkins *et al.*,[12] enter the vacuum-isolated ionization region through a skimmer[13] where they are ionized by an 193-nm ArF laser focused to an intensity of approximately $10^8$ W/cm$^2$ between the first two plates of a three-element grid system.[14] The cluster output of the source is monitored by recording the full-beam arrival at the detector, located 1.25 m downstream. A typical mass scan for silicon, with the focusing elements (Fig. 1) set to optimize collection of small to medium clusters at the detector, is shown in the lower portion of Fig. 2. The measured distribution envelope of cluster sizes depends on the settings of the deflecting elements, the choice of source carrier gas and pressures, and the intensity of the ionizing laser. The relative production of cluster sizes is independent of whether ArF (6.4 eV) or KrF (5.0 eV) is used as the ionizing laser, although the total flux of clusters is much larger with ArF.

A set of "switch-out" electrodes is installed halfway down to the time-of-flight region and operates as a fast valve, allowing only clusters with the mass of interest to proceed further. The chosen cluster group is slowed by the deacceleration grids and exposed to an intense beam of 267-, 355-, or 532-nm pulsed-laser radiation. The resulting charged photofragments are

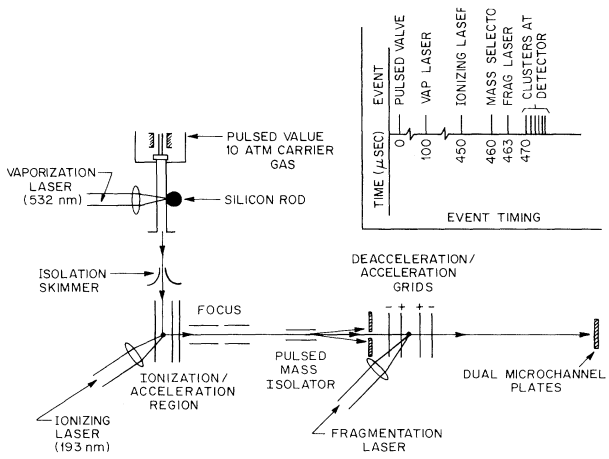


FIG. 1. Experimental apparatus: Clusters are grown from vaporized Si in the source, converted to cluster ions, and dispersed according to mass after acceleration. A single mass is isolated, fragmented with a laser, and the separated fragments are detected on the microchannel plates.

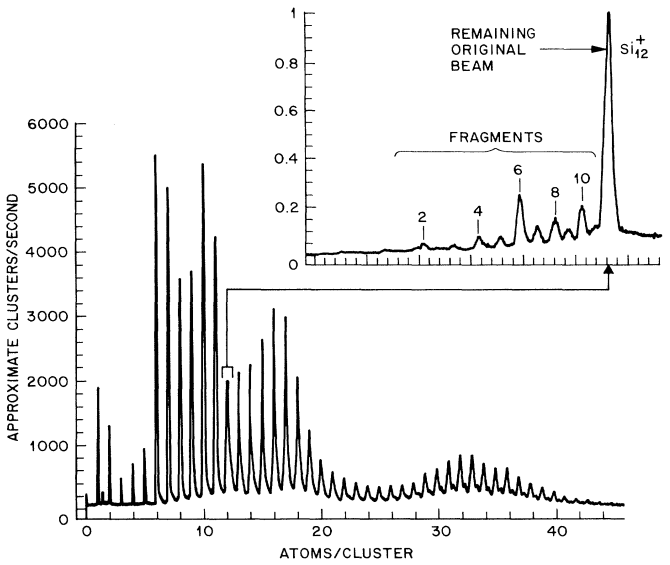


FIG. 2. A spectrum of small to medium cluster ions. An example of the preselection of cluster size is shown on the upper right where a single ion mass, $Si_{12}^+$, is isolated and fragmented with 266-nm radiation to produce the fragmentation spectrum shown on the upper right.

reaccelerated and dispersed in the second half of the time-of-flight region. The inset of Fig. 2 displays the fragmentation spectra obtained when $Si_{12}^+$ is isolated by the "switch-out" plates and photofragmented by a saturation fluence of 266-nm light.

The recorded fragmentation spectra for any cluster size depends critically on how well the laser beam overlaps the cluster packet. This experimental difficulty is largely overcome by explicitly measuring the laser intensity dependence of the separate fragmentation channels for *each* cluster size. For those channels that show a low-intensity linear dependence of signal on light intensity, a relative cross section for direct fragmentation can be readily extracted. Alternatively, a complete "family tree" for the breakup of any $Si_n^+$ for an arbitrary intensity can be constructed by analyzing all the data starting with $Si_2^+$ and working up to $Si_n^+$. Such an analysis indicates, for example, that the fragmentation pattern for $Si_{12}^+$ at high intensity, shown in the inset of Fig. 2, arises from saturation of the primary fragmentation of $Si_{12}^+$ into $Si_{10}^+$ with subsequent fragmentation of $Si_{10}^+$ into $Si_6^+$.

The relative cross sections for primary photofragmentation at 532 nm of $Si_n^+ \rightarrow Si_m^+$ for $n = 2$ to 12 ($m < n$) are shown in Table I. These values for a given $n$ are found to be largely independent of whether the fragmentation-laser photon energy is 2.3, 3.5, or 4.7 eV, although the absolute cross sections are considerably larger at 4.7 eV than at 2.3 eV.

Figure 3 shows the relative *total* photofragmentation cross sections for $Si_n^+$ for $n = 2$ to 11 at 532 nm. These values are the cross sections for photofragmentation of $Si_n^+$ summed over all fragmentation channels, and are measured by recording the saturation in the depletion of the original beam of $Si_n^+$ as a function of laser intensity. For this measurement the apparatus is programmed to record simultaneously the various $Si_n^+$ cross sections relative to that of $Si_6^+$, thus avoid-

TABLE I. Branching ratios for the fragmentation of $Si_n^+$ initial states into $Si_m^+$ final states.

| FINAL CLUSTER \ INITIAL CLUSTER | $Si_2^+$ | $Si_3^+$ | $Si_4^+$ | $Si_5^+$ | $Si_6^+$ | $Si_7^+$ | $Si_8^+$ | $Si_9^+$ | $Si_{10}^+$ | $Si_{11}^+$ | $Si_{12}^+$ |
|---|---|---|---|---|---|---|---|---|---|---|---|
| $Si^+$ | 1.00 | 0.25(3) | 0.17(3) | 0.05(1) | 0.00(1) | 0.01(1) | 0.00(1) | 0.00(1) | 0.00(1) | 0.00(1) | 0.00(1) |
| $Si_2^+$ | | 0.75(3) | 0.18(3) | 0.05(1) | 0.04(1) | 0.02(1) | 0.01(1) | 0.00(1) | 0.00(1) | 0.00(1) | 0.02(1) |
| $Si_3^+$ | | | 0.65(5) | 0.08(1) | 0.05(1) | 0.01(1) | 0.01(1) | 0.02(1) | 0.01(1) | 0.02(1) | 0.00(1) |
| $Si_4^+$ | | | | 0.82(2) | 0.21(2) | 0.03(1) | 0.07(2) | 0.06(2) | 0.09(2) | 0.09(2) | 0.05(2) |
| $Si_5^+$ | | | | | 0.70(4) | 0.11(2) | 0.07(2) | 0.08(2) | 0.03(2) | 0.13(3) | 0.05(2) |
| $Si_6^+$ | | | | | | 0.82(2) | 0.28(4) | 0.39(3) | 0.64(4) | 0.29(3) | 0.05(2) |
| $Si_7^+$ | | | | | | | 0.55(4) | 0.19(3) | 0.12(3) | 0.36(4) | 0.08(2) |
| $Si_8^+$ | | | | | | | | 0.26(4) | 0.07(2) | 0.04(2) | 0.12(3) |
| $Si_9^+$ | | | | | | | | | 0.04(2) | 0.03(2) | 0.09(2) |
| $Si_{10}^+$ | | | | | | | | | | 0.04(2) | 0.42(5) |
| $Si_{11}^+$ | | | | | | | | | | | 0.13(3) |

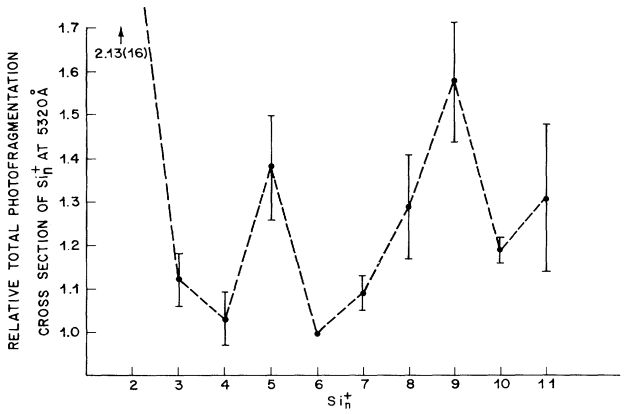


FIG. 3. Relative total photofragmentation cross sections of $Si_n^+$ at 532 nm. $Si_6^+$ is used as a reference. The absolute total photofragmentation cross section for $Si_6^+$ is $7(3) \times 10^{-19}$ cm$^{-2}$.

ing most of the systematic errors associated with absolute cross-section measurements. The absolute total photofragmentation cross section for $Si_6^+$ was determined in a separate experiment in which detailed measurements of the laser power, spot size, and overlap with the cluster packet were performed. This value is $7(3) \times 10^{-19}$ cm$^{-2}$ at 532 nm, comparable to previous measurements of photodissociation cross sections in ions,[15] but larger than typical values for nonresonant photoionization cross sections. Thus, substantial photofragmentation is likely to occur during the photoionization process.

Table I and Fig. 3 support several important observations about the photofragmentation of $Si_n^+$. Table I shows that when the initial ionic cluster breaks up, the positive charge remains predominantly on the larger fragment and, for breakup of clusters with $n = 7$–11, the fragment $Si_6^+$ is unusually prominent. Figure 3 shows that $Si_4^+$, $Si_6^+$, and $Si_{10}^+$ have relatively small total photofragmentation cross sections, and are presumably more tightly bound than other $Si_n^+$ that differ by one constant atom, e.g., $Si_5^+$ and $Si_9^+$.

Other than the early work of Honig,[16] and recent laser-stimulated desorption studies of Tsong,[5] Si clusters have not been studied experimentally. Honig formed $Si_n$ in an oven above molten silicon and measured relative numbers of *neutral* $Si_n$ up to $Si_6$. His data are in remarkable agreement with the relative stability of $Si_n^+$, $n \leq 6$, clusters inferred from the data displayed in Fig. 3.

Recently, calculations of the equilibrium geometries of small clusters ($n < 6$) of Ge[17] and Si[18] have been attempted which suggest that, unlike carbon, the small microclusters of Si and Ge are not linear. While the exact form of the geometries for $n = 3$–6 is not established, the microcrystals are believed to be relatively compact, reconstructed subunits, viz., triangle, rhombus, trigonal bipyramid, and distorted trigonal bipyramid ($n = 6$). To our knowledge, there exist no calculations of either ionic or neutral Si or Ge clusters geometries for $n > 6$.

Because the *relative* photofragmentation cross sections of $Si_n^+$ are found to be independent of the wavelength of the fragmenting light, the mass dependence of the cross sections is assumed to reflect the relative stability of the clusters. One is then tempted to propose models of the geometries of $Si_n^+$ clusters for $n > 6$ which are consistent with our fragmentation data. A particularly simple, though probably naive, model is one in which the Si atoms are configured as microcrystals of a tetrahedral diamond lattice, and the photofragmentation of these microcrystals occurs preferentially along ⟨111⟩ directed bonds. The essential structures in this model are the reconstructed six-membered "chair" ring and the ten-membered microcrystal subunit of the tetrahedral diamond lattice ("adamantane cage"). The six-membered complex is the most tightly bound unit and is a prominent fragment in the breakup of larger clusters. It is envisioned visioned to fragment from larger clusters as a "chair" ring which reconstructs into a compact symmetric unit; most probably a distorted trigonal bipyramid.[18] Geometries of clusters larger than six are obtained by adding successive atoms to this structure in some (as yet) undetermined manner. At $n = 10$, a highly symmetric three-dimensional complex results. It may well be that the geometry of this complex is substantially different from a crystal subunit (i.e., heavily reconstructed), but this simple model envisions the $n = 10$ unit to contain four equivalent six-membered rings. It is again tightly bound, and is a common fragment in the breakup of larger clusters.

Although this model of equilibrium geometries and preferential bond fragmentation is not unique, it accounts for the photofragmentation data of the larger $Si_n^+$ clusters in a natural way. For example, the model predicts that $Si_{10}^+$ is more tightly bound than $Si_9^+$ or $Si_{11}^+$, and that it should fragment primarily along ⟨111⟩ bonds into $Si_6^+$ and $Si_4$. This prediction is borne out by the data of Fig. 3 and Table I. For $Si_{11}^+$ the predicted structure is shown in Fig. 4(a). [The placement of the eleventh atom (shaded in Fig. 4) is undetermined, other than being attached to the core $Si_{10}$.] According to the model, photofragmentation should be dominated by fragments resulting from the two breakup patterns (6+5 and 7+4) shown in Fig. 4(b) and 4(c). Figure 4(d) and 4(e) show how the fragmented six-membered ring can readily reconstruct into a compact equilibrium geometry. Table I indicates that clusters with four, five, six, and seven atoms do indeed dominate the photofragmentation spectra of $Si_n^+$

In conclusion, we have measured the photofragmen-

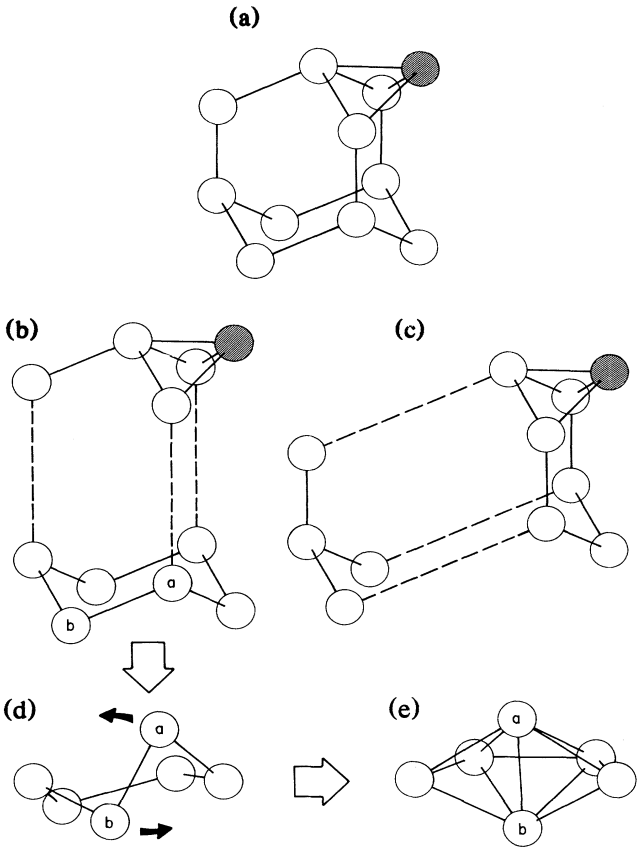


FIG. 4. (a) A possible structure for $Si_{11}^{+}$ showing fragmentation paths to $Si_{4-7}^{+}$ (b),(c). The placement of the eleventh atom (shaded) is uncertain. (d),(e) A possible bond-rotation mechanism by which the six-membered "chair" ring can reconstruct into a distorted trigonal bipyramid is shown.

tation spectra of $Si_n^+$ for $n = 2$–12 and have shown that a model of Si cluster geometries based on microcrystals is consistent with the data. The apparatus used in these experiments is capable of examining many physical properties of clusters, including measurements which are in progress of the mass dependence of charge exchange.

We would like to thank R. E. Smalley and his coworkers for detailed consultations on the laser-vaporization source, and P. H. Citrin, J. C. Phillips, and J. Bokor for helpful discussions.

[1]P. W. Stephens and J. C. King, Phys. Rev. Lett. **51**, 1538 (1983).

[2]I. A. Harris, R. S. Kidwell, and J. A. Northby, Phys. Rev. Lett. **53**, 2390 (1984).

[3]A. Ding and J. Hesslich, Chem. Phys. Lett. **94**, 54 (1983).

[4]O. Echt, K. Sattler, and E. Recknagel, Phys. Rev. Lett. **47**, 1121 (1981).

[5]T. T. Tsong, Appl. Phys. Lett. **45**, 1149 (1984).

[6]E. A. Rohlfing, D. M. Cox, and A. Kaldor, J. Chem. Phys. **81**, 3322 (1984).

[7]W. D. Knight, K. Clemenger, W. A. de Heer, W. A. Saunders, M. Y. Chou, and M. L. Cohen, Phys. Rev. Lett. **52**, 2141 (1984).

[8]M. M. Kappes, R. W. Kunz, and E. Schumacher, Chem. Phys. Lett. **91**, 413 (1982).

[9]U. Buck and H. Meyer, Phys. Rev. Lett. **52**, 109 (1984).

[10]A. van Lumig and J. Reuss, Int. J. Spectrom. Ion Phys. **25**, 137 (1977), and **27**, 197 (1978).

[11]M. F. Jarrold, A. J. Illies, and M. T. Bowers, J. Chem. Phys. **81**, 214 (1984).

[12]J. B. Hopkins, P. R. R. Langridge-Smith, M. D. Morse, and R. E. Smalley, J. Chem. Phys. **78**, 1627 (1983).

[13]Beam Dynamics, Inc., Minneapolis, Minnesota.

[14]W. C. Wiley and I. H. McLaren, Rev. Sci. Instrum. **26**, 1150 (1951).

[15]G. P. Smith and L. C. Lee, J. Chem. Phys. **69**, 5393 (1978).

[16]R. E. Honig, J. Chem. Phys. **22**, 1610 (1954).

[17]J. Koutechy and G. Pacchioni, Ber. Bunsenges. Phys. Chem. **88**, 233 (1984); G. Pacchioni and J. Koutechy, Ber. Bunsenges. Phys. Chem. **88**, 242 (1984).

[18]K. Raghavachari (AT&T Bell Laboratories, Murray Hill, N.J.), private communication.